

UNC-51/ATG1 kinase regulates axonal transport by mediating motor–cargo assembly

Hirofumi Toda,^{1,2,6} Hiroaki Mochizuki,^{2,6} Rafael Flores III,¹ Rebecca Josowitz,³ Tatiana B. Krasieva,⁴ Vickie J. LaMorte,⁴ Emiko Suzuki,⁵ Joseph G. Gindhart,³ Katsuo Furukubo-Tokunaga,^{2,8} and Toshifumi Tomoda^{1,7}

¹Division of Neurosciences, Beckman Research Institute of the City of Hope, California 91010, USA; ²Graduate School of Life and Environmental Sciences, University of Tsukuba, Tsukuba 305-8572, Japan; ³Department of Biology, University of Richmond, Virginia 23173, USA; ⁴Beckman Laser Institute, University of California at Irvine, Irvine, California 92697, USA; ⁵Gene Network Laboratory, National Institute of Genetics, Mishima, Shizuoka 411-8540, Japan

Axonal transport mediated by microtubule-dependent motors is vital for neuronal function and viability. Selective sets of cargoes, including macromolecules and organelles, are transported long range along axons to specific destinations. Despite intensive studies focusing on the motor machinery, the regulatory mechanisms that control motor–cargo assembly are not well understood. Here we show that UNC-51/ATG1 kinase regulates the interaction between synaptic vesicles and motor complexes during transport in *Drosophila*. UNC-51 binds UNC-76, a kinesin heavy chain (KHC) adaptor protein. Loss of *unc-51* or *unc-76* leads to severe axonal transport defects in which synaptic vesicles are segregated from the motor complexes and accumulate along axons. Genetic studies show that *unc-51* and *unc-76* functionally interact *in vivo* to regulate axonal transport. UNC-51 phosphorylates UNC-76 on Ser¹⁴³, and the phosphorylated UNC-76 binds Synaptotagmin-1, a synaptic vesicle protein, suggesting that motor–cargo interactions are regulated in a phosphorylation-dependent manner. In addition, defective axonal transport in *unc-76* mutants is rescued by a phospho-mimetic UNC-76, but not a phospho-defective UNC-76, demonstrating the essential role of UNC-76 Ser¹⁴³ phosphorylation in axonal transport. Thus, our data provide insight into axonal transport regulation that depends on the phosphorylation of adaptor proteins.

[*Keywords:* Axonal transport; *unc-51*; kinesin adaptor; phosphorylation; motor–cargo assembly]

Supplemental material is available at <http://www.genesdev.org>.

Received March 10, 2008; revised version accepted October 10, 2008.

The axon serves as a track for long-distance transport of synaptic components that are synthesized within cell soma and delivered to nerve terminals (for reviews, see Brady 1991; Vallee and Sheetz 1996; Guzik and Goldstein 2004). The microtubule (MT) transport system supports most axonal traffic, in which kinesins are the major anterograde motors responsible for the transport of a wide range of cargoes (i.e., synaptic vesicles [SVs], mitochondria, cytoskeletal elements, and mRNAs), whereas dyneins are responsible for the retrograde transport of cargoes (Hirokawa 1998; Vale 2003).

A number of transport components have been identified, and the recent discovery of a large family of structurally related motor proteins has addressed the question

of motor–cargo specificity (Miki et al. 2005). The kinesin superfamily proteins (KIFs) are comprised of >30 members, and each KIF is responsible for carrying a specific subset of cargoes. In addition, protein–protein interaction screens with several motor proteins have identified multiple adaptor proteins, which further determine the specificity of cargoes transported by each motor (Guzik and Goldstein 2004; Hirokawa and Takemura 2005). For example, *Drosophila* kinesin heavy chain (KHC), the catalytic component of kinesin-1, binds an adaptor, Milton, that specifically recruits mitochondria as cargo and transports them toward synapses (Stowers et al. 2002). KHC also binds UNC-76/FEZ1, an evolutionarily conserved adaptor protein (Bloom and Horvitz 1997; Kuroda et al. 1999; Blasius et al. 2007), and loss of *unc-76* results in defective SV transport in *Drosophila* segmental nerves (SGNs) (Gindhart et al. 2003). Kinesin light chain (KLC) interacts with a scaffolding protein c-Jun N'-terminal kinase-interacting protein 1 (JIP1) (Verhey et al. 2001; Horiuchi et al. 2005) or an additional scaffolding protein

⁶These authors contributed equally to this work.
Corresponding authors.

⁷E-MAIL ttomoda@coh.org; FAX (626) 446-5774.

⁸E-MAIL tokunaga@sakura.cc.tsukuba.ac.jp; FAX 81-298-53-6644.

Article is online at <http://www.genesdev.org/cgi/doi/10.1101/gad.1734608>.

UNC-16/SYD/JIP3 (c-Jun N'-terminal kinase-interacting protein 3) in *Caenorhabditis elegans*, *Drosophila*, and mammals (Bowman et al. 2000; Byrd et al. 2001; Verhey et al. 2001). JIP1 in turn binds amyloid precursor protein (APP) (Scheinfeld et al. 2002), a kinesin-1 cargo that is implicated in normal axonal transport and in Alzheimer's disease (Torroja et al. 1999; Kamal et al. 2001; Lazarov et al. 2005).

Despite this progress in understanding motor-cargo specificity, it is not well understood how motor-cargo assembly is regulated during transport. Many components of the axonal transport machinery, such as kinesins, are phosphoproteins (Hollenbeck 1993), suggesting that phosphorylation may play a role in axonal transport. Recent reports have addressed the roles of glycogen synthase kinase 3 β (GSK3 β), c-Jun N'-terminal kinase (JNK) and Ca²⁺-calmodulin kinase II (CaMKII), which negatively impact motor-cargo assembly during transport (Morfini et al. 2002; Horiuchi et al. 2007; Guillaud et al. 2008). However, little is known about the mechanisms of how organelle motility is dynamically controlled or maintained in vivo.

Members of the conserved Ser/Thr kinase UNC-51 family (*unc-51/Unc51.1/Unc51.2*) are key regulatory genes that control axonal elongation during nervous system development in *C. elegans* and mice (Hedgecock et al. 1985; Ogura et al. 1994; Tomoda et al. 1999; Zhou et al. 2007). Murine *Unc51.1* is expressed in a number of neuronal populations during development, including cerebellar granule cells, in which *Unc51.1* is localized to both elongating axonal shafts and growth cones. Inhibition of *Unc51.1* activity leads to retarded neurite extension and parallel fiber formation in cerebellar granule neurons (Tomoda et al. 1999). A recent study showed that axon formation is regulated by the endocytic membrane traffic pathway via an *Unc51.1*-containing protein complex (*Unc51.1/SynGAP/Rab5/Syntenin*) (Tomoda et al. 2004). UNC-51 also interacts with VAB-8, which contains a kinesin-motor like domain, and these proteins cooperatively regulate axon extension in *C. elegans* (Lai and Garriga 2004). In addition, UNC-14, a protein that interacts with UNC-51 (Ogura et al. 1997), plays a role in kinesin-1-dependent axonal transport in *C. elegans* (Sakamoto et al. 2005). Furthermore, *unc-51* mutants in *C. elegans* manifest abnormal accumulation of intrasomal vesicles that are positive for UNC-5, a Netrin/UNC-6 receptor (Ogura and Goshima 2006), suggesting a role for UNC-51 in anterograde vesicle transport. Collectively, these lines of evidence suggest that UNC-51 plays a role in intracellular transport.

In this study, we demonstrate a role for UNC-51-mediated phosphorylation in the regulation of axonal transport in vivo. Loss of *unc-51* results in defective axonal transport in a cargo type-dependent manner. UNC-51 binds and phosphorylates the kinesin adaptor UNC-76. When phosphorylated at Ser¹⁴³, UNC-76 has an elevated affinity for Synaptotagmin-1 (Syt-1), a major transmembrane protein of SVs (Südhof 2004), whereas non-phospho-UNC-76 fails to bind Syt-1. Characterization of *unc-51* therefore reveals a key step in the regulation of

motor-cargo interaction and provides insight into the dynamic control of axonal transport in vivo.

Results

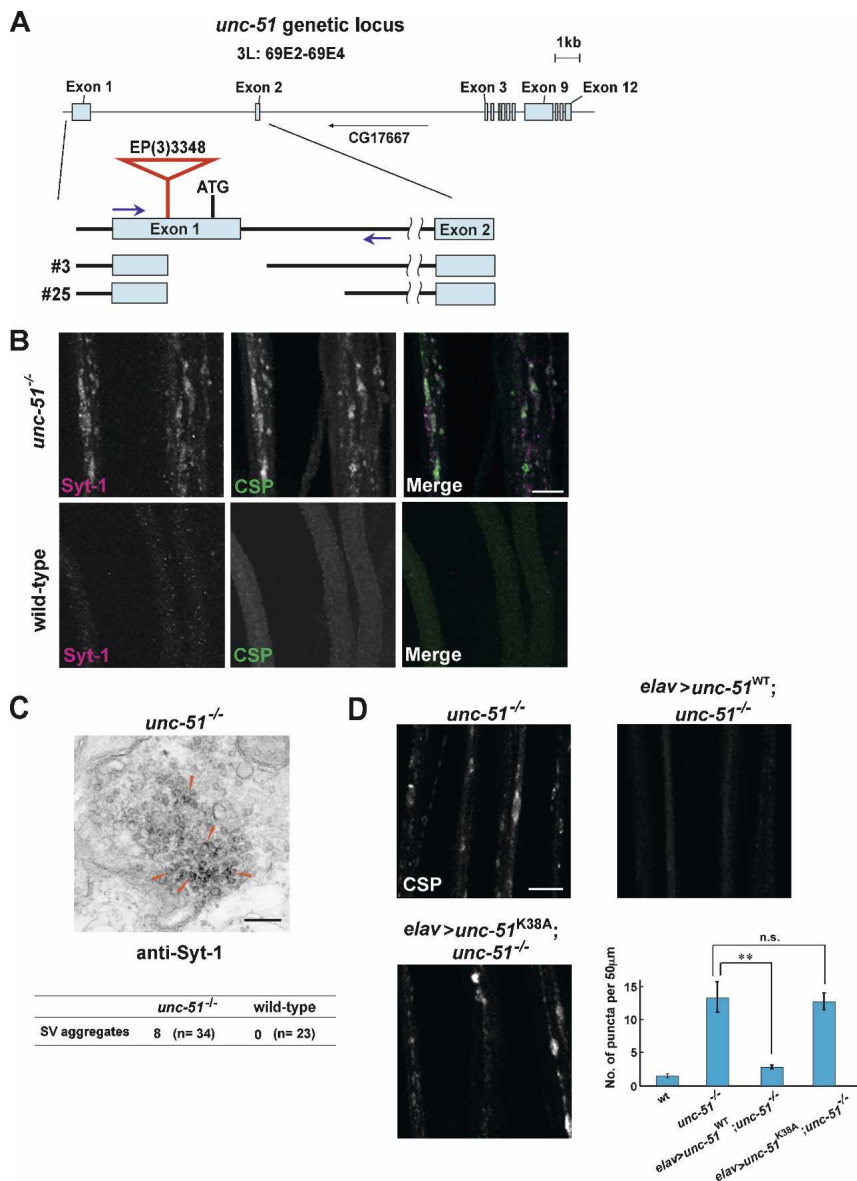
Generation of *unc-51*-null mutants in *Drosophila*

The Ser/Thr kinase UNC-51 is implicated in axonal development in *C. elegans* and mice (Ogura et al. 1994; Tomoda et al. 1999; Zhou et al. 2007). The *Drosophila* genome has a single *unc-51* homolog (CG10967), which is also referred to as *atg1* (Scott et al. 2007) or *Pegarn* (Ahantari et al. 2008). Expression analysis of *unc-51* mRNA in situ in *Drosophila* revealed that it was widely distributed throughout stage 2 embryos, demonstrating a high level of maternal expression (Supplemental Fig. S1A). The *unc-51* mRNA continued to be expressed throughout the embryonic stages, and was progressively restricted to the nervous system, suggesting a role for *unc-51* in neuronal development. To further elucidate the neuronal functions of *unc-51*, we generated null alleles in *Drosophila*. P-element EP{3}3348 is a semilethal insertion at adult stage and is inserted within the first exon of the *unc-51* gene, 539 base pairs (bp) upstream of the ATG initiation codon (Fig. 1A). Precise excision of this P-element rescued the semilethality (data not shown). Two *unc-51* mutant alleles, *unc-51*³ and *unc-51*²⁵, were generated by imprecise excision, which deleted 804 bp and 1787 bp, respectively, downstream from the insertion point (Fig. 1A), removing part of the first exon, including the ATG initiation codon. These mutations caused axonal transport defects at the larval stage, as well as pupal lethality, and failed to complement each other. Genetic crosses of *unc-51*³ or *unc-51*²⁵ with an *unc-51* deficiency line [*unc-51*³/*Df(3L)ED4486* or *unc-51*²⁵/*Df(3L)ED4486*] gave rise to phenotypes identical to *unc-51*³/*unc-51*²⁵, displaying both defective axonal transport and pupal lethality. Immunohistochemical analyses confirmed loss of UNC-51 protein expression in the mutants (Supplemental Fig. S1B). Thus, the evidence indicates that both alleles are null for the *unc-51* locus.

Phenotypic analysis of axon development in *unc-51* mutants

Consistent with previous studies on the role of *unc-51* in axon formation in worms and mice (Ogura et al. 1994; Tomoda et al. 1999), *Drosophila unc-51* mutants exhibited varying degrees of defective axonal tracts in the ventral nerve cord (VNC) at the embryonic stage, including premature truncation and abnormal midline crossing of longitudinal tracts (H. Mochizuki, H. Toda, T. Tomoda, and K. Furukubo-Tokunaga, unpubl.). Approximately 47% of the mutants were estimated to be dead by the early third instar larval stage, likely due to defective axon formation during the embryonic period. In contrast, the remainder (~53%) survived through the larval stage, with the SGNs of third instar larvae extended (Supple-

Figure 1. *unc-51* functions in axonal transport. (A) Molecular structures of the *unc-51*-null mutant alleles. P-element EP(3)3348 is inserted within the first exon of the *unc-51* gene, 539 bp upstream of the initiation ATG codon. Two *unc-51*-null alleles, *unc-51*³ and *unc-51*²⁵, were generated by imprecise excision. PCR amplification of these *unc-51* alleles (blue arrows indicate locations of primers) and subsequent sequencing analyses confirmed that *unc-51*³ has an 804 bp deletion and *unc-51*²⁵ has a 1787-bp deletion. Both alleles lack the start codon, and did not affect the expression unit of CG17667 located within intron 2. (B) SGNs of *unc-51*-null mutant (*unc-51*³/*unc-51*²⁵) or wild-type third instar larvae immunostained with anti-Syt-1 (red) and anti-CSP (green). Syt-1-positive aggregates colocalized with those positive for CSP in *unc-51* mutants. Bar, 10 μ m. (C) Ultrastructure of SV aggregates in *unc-51* mutants. Electron micrograph of a cross-section of an *unc-51* mutant SGN immunostained with anti-Syt-1. Arrowheads indicate SVs positive for anti-Syt-1. (Table) The number of SV aggregates (defined as a cluster of >20 SVs per aggregate) was scored in electron-micrographs from *unc-51* mutants ($n = 34$) and wild type ($n = 23$). Bar, 200 nm. (D) Genetic rescue of axonal transport defect in *unc-51* mutants by *unc-51* transgene. CSP-positive SV aggregation phenotype in *unc-51* mutants was rescued by pan-neuronal expression of *unc-51*/wild-type transgene (*elav*^{c155} > UAS-*unc-51*^{WT}; *unc-51*³/*unc-51*²⁵), but not by a kinase-deficient *unc-51* (*elav*^{c155} > UAS-*unc-51*^{K38A}; *unc-51*³/*unc-51*²⁵). Numbers of CSP-positive puncta per 50 μ m SGN (mean \pm SEM) were plotted for each genotype (graph). (**). Statistically significant rescue ($P < 0.01$, Student *t* test). (n.s.) Not significant ($P = 0.843$). Bar, 10 μ m.



mental Fig. S1C) and connected to normal muscle targets (data not shown), and died during the pupal stage. Electron microscopy (EM) analysis of SGN cross-sections at the third instar stage revealed that the number of axons per SGN and the average axon caliber in mutant larval SGNs was indistinguishable from wild type (Supplemental Fig. S1D), suggesting that *unc-51* mutants that survive to larval stage have little anatomical abnormality in axon formation.

Selective membrane localization defects in *unc-51* mutant larvae

Because recent studies in worms and mice suggested a role for *unc-51*-mediated membrane organization in axon formation (Tomoda et al. 2004; Ogura and Goshima 2006), we tested several membrane markers to identify

potential membrane defects within extended SGNs of *unc-51* mutant third instar larvae. We observed aberrant accumulation of SVs within mutant SGNs, as evidenced by prominent aggregation of Syt-1 (Fig. 1B). This elevated level of Syt-1 in mutant SGNs correlated with fewer numbers of synaptic boutons, less intense Syt-1 immunostaining, reduced bouton area, and reduction in total amount of Syt-1 at neuromuscular junctions (NMJ) (segment A2, muscle 6/7) as compared with the wild type (Supplemental Fig. S2). An additional SV marker, cysteine string protein (CSP) (Zinsmaier et al. 1994), confirmed the phenotype by showing a nearly complete overlap in localization with Syt-1-positive aggregates in *unc-51* mutants (Fig. 1B). Immuno-EM revealed that Syt-1-positive aggregates were comprised of clusters of SVs within the axon shaft (Fig. 1C). The SV transport defect in *unc-51* mutants was rescued by *unc-51* transgene expression

(*elav^{c155} > UAS-unc-51;unc-51³/unc-51²⁵*), attributing the mutant phenotype to the loss of *unc-51* activity (Fig. 1D). A kinase-deficient *unc-51* transgene carrying a point mutation in the ATP-binding site failed to rescue the mutant phenotype (*elav^{c155} > UAS-unc-51^{K38A};unc-51³/unc-51²⁵*), demonstrating a critical role for the kinase activity in organizing axonal membranes (Fig. 1D).

To further address the selectivity of membrane types affected by *unc-51* mutation, additional markers were tested. Rab5, an early endosomal marker, showed mild aggregates within mutant SGNs, in a pattern distinct from those of CSP-positive SVs (Supplemental Fig. S3A). A late endosome–lysosome marker, LAMP1, revealed many aggregates, some of which colocalized with SV aggregates (Supplemental Fig. S3B). In contrast, overall mitochondrial localization appeared unaffected in mutants and rarely overlapped with Syt-1 (Supplemental Fig. S3C), suggesting that SV aggregates do not serve as physical barriers for mitochondrial transport and that SV and mitochondria have distinct transport pathways. Quantitative analysis confirmed that the overall distribution of the sizes of mito::GFP-positive puncta smaller than 20 μm^2 were equivalent between wild type and *unc-51* mutants (Supplemental Fig. S3D), although more large puncta (>20 μm^2) were present in *unc-51* mutants (Supplemental Fig. S3E), suggesting that mitochondrial transport is also affected in *unc-51* mutants. Indeed, time-lapse video microscopic analysis of mitochondria labeled with mito::GFP (*OK6 > UAS-mito::GFP*) revealed that mitochondria in wild type moved at an average speed of $0.25 \pm 0.02 \mu\text{m}/\text{sec}$ ($n = 27$), whereas those in *unc-51* mutants moved at $0.16 \pm 0.02 \mu\text{m}/\text{sec}$ on average ($n = 36$) (Supplemental Movie S1). Thus, the *unc-51* mutation results in a varying degree of axonal membrane defects in a cargo type-dependent manner.

In EM analysis, we observed clusters of a variety of membrane components within *unc-51* mutant axons more frequently than in wild type. Those include dense core vesicles, multivesicular bodies (Supplemental Fig. S1E) and small clear vesicles that were reminiscent of SVs (Fig. 1C). Taken together, these results suggest that *unc-51* is important for organizing axonal membranes in the larval SGNs.

unc-51 functions in SV transport

The SV aggregation in *unc-51* mutants (Fig. 1B) was reminiscent of that reported for mutants of *Kinesin heavy chain* (*Khc*) (Hurd and Saxton 1996), *Kinesin light chain* (*Klc*) (Gindhart et al. 1998), and *Dynein heavy chain* (*Dhc*) (Martin et al. 1999). As in these mutants, *unc-51* mutants displayed sluggish larval crawling and occasional tail flipping (data not shown), a phenotype consistent with defective axonal transport. SVs are primarily generated in neuronal soma and delivered to synapses via anterograde transport machinery. To visualize SV transport defects in *unc-51* mutant SGNs, time-lapse video microscopy was performed (Supplemental Movie S2). In wild-type third instar larvae (*OK6 > UAS-Syt-1::eGFP*), most vesicles labeled with Syt-1::eGFP moved at velocities typical of normal axonal transport (as fast as 2.26 $\mu\text{m}/\text{sec}$; average $0.89 \pm 0.06 \mu\text{m}/\text{sec}$, $n = 47$) with 53.2% of vesicles moving anterogradely and 46.8% moving retrogradely, in good agreement with a recent study (Barkus et al. 2008). In contrast, prominent accumulations of Syt-1::eGFP-positive vesicles were observed in *unc-51* mutants, and ~95% of small individual puncta outside aggregates were immobile or moved slower than 0.2 $\mu\text{m}/\text{sec}$ during the observation period (30 sec). Less than 5% of the Syt-1::eGFP-positive vesicles were mobile and the average speed of SV transport in *unc-51* mutants was $0.05 \pm 0.01 \mu\text{m}/\text{sec}$ ($n = 62$) (Supplemental Movie S2). Therefore, *unc-51* plays a significant role in SV transport at larval stages.

unc-51 genetically interacts with components of kinesin-1-dependent axonal transport

Given that *unc-51* functions in SV transport, we investigated a potential genetic interaction of *unc-51* with several genes previously implicated in axonal transport by testing for SV transport defects. Among those, *unc-76* (Gindhart et al. 2003) and *Klc* showed a genetic interaction with *unc-51* in a double heterozygous scheme (*unc-76^{+/-};unc-51^{+/-}* or *Klc^{+/-};unc-51^{+/-}*) (Fig. 2; Supplemental Fig. S4), a condition often used to identify functional interactions among transport genes (Martin et al. 1999).

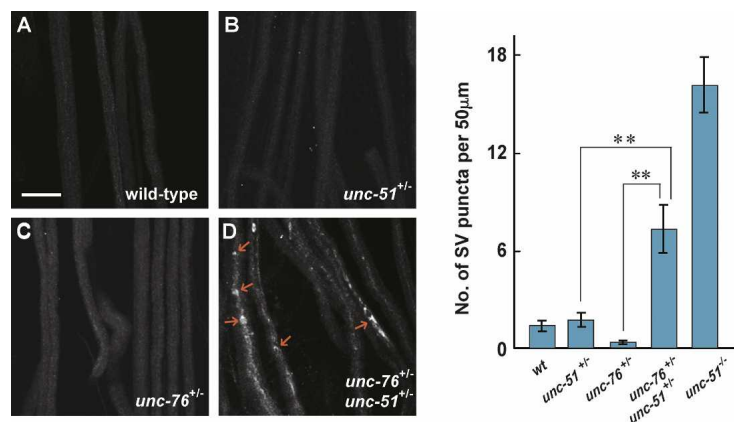


Figure 2. *unc-51* genetically interacts with *unc-76* in axonal transport. SGNs of wild type or the indicated mutants immunostained with anti-CSP at the third instar larval stage. Arrows show CSP-positive aggregates. Bar, 20 μm . The number of aggregates found per 50 μm of nerve shaft was scored for each genotype (graph). Statistical significance evaluated by Student *t* test. (***) $P < 0.01$. Error bars show \pm SEM. Genotypes are w (A), *unc-51³/+* (B), *unc-76^{Df(1)107}/+* (C), and *unc-76^{Df(1)107}/+;unc-51³/+* (D).

UNC-76 is a KHC adaptor protein that is necessary for kinesin-1-mediated axonal transport (Gindhart et al. 2003), and KLC is an accessory component of kinesin-1 (Gindhart et al. 1998). Quantitative analysis revealed that *unc-76^{+/-}unc-51^{+/-}* double heterozygotes had more SV aggregates (~7/50 μ m) than *unc-76^{+/-}* or *unc-51^{+/-}* single heterozygotes (<2/50 μ m) (Fig. 2, graph). Likewise, *Klc^{+/-}unc-51^{+/-}* double heterozygotes had significantly more SV aggregates as compared with *Klc^{+/-}* or *unc-51^{+/-}* single heterozygotes (Supplemental Fig. S4, graph). In contrast, *Khc*, *Dhc*, *unc-104 (imac)* (Pack-Chung et al. 2007), *sunday driver (syd)* (Bowman et al. 2000), *Lis-1* (Liu et al. 2000), and *Aplip1* (Horiuchi et al. 2005) showed no obvious interaction with *unc-51* (Supplemental Fig. S4, graph). This suggests that *unc-51*-dependent regulation of axonal transport involves components that are implicated in kinesin-1-mediated organelle transport.

UNC-51 forms a complex with KHC via UNC-76

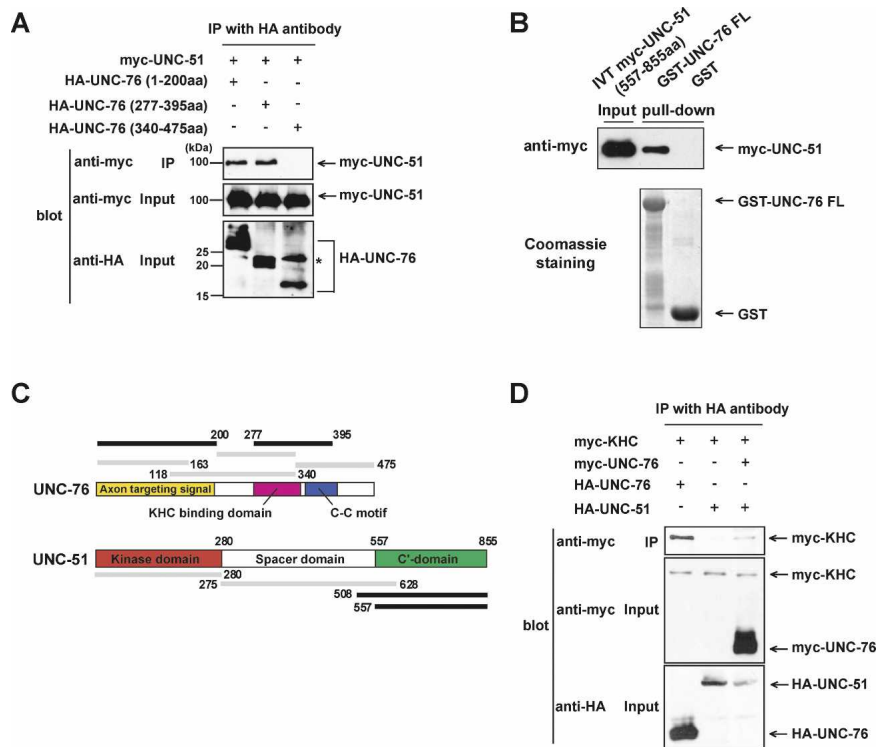
To provide mechanistic insight into how *unc-51* functions in kinesin-1-mediated transport, we examined the physical interaction between UNC-51 and UNC-76 or KLC. Although UNC-51 did not bind KLC (data not shown), UNC-51 bound UNC-76 in coimmunoprecipitation assays in HEK293T cells. Additional coimmunoprecipitation assays using a series of UNC-51 and UNC-76 deletion constructs revealed that the C'-terminal tail of

UNC-51 bound to the UNC-76 N'-terminal domain, which targets UNC-76 to axons (Bloom and Horvitz 1997), and also bound to the UNC-76 C'-terminal domain, which contains a coiled-coil motif (Fig. 3A; Supplemental Fig. S5) indicating that UNC-76 binds UNC-51 in a bipartite fashion. GST pull-down experiments confirmed a direct interaction between UNC-51 and UNC-76 (Fig. 3B). Association domains of UNC-51 and UNC-76 are summarized in Figure 3C. Moreover, UNC-51 was able to precipitate KHC in the presence of UNC-76 in coimmunoprecipitation assays (Fig. 3D). Therefore, we hypothesized that UNC-51 plays a role in kinesin-1-dependent axonal transport by interacting with UNC-76.

Disorganized motor-cargo localization in *unc-51* mutants

To further investigate the role of *unc-51* in kinesin-1-dependent axonal transport, we first examined potential defects of MTs in *unc-51* mutants. Localization of a MT-associated protein, MAP1B, appeared unaffected in *unc-51* mutant SGNs (Supplemental Fig. S6A), and a MT-kinesin cosedimentation assay showed that the MT-kinesin association is maintained in *unc-51* mutants (Supplemental Fig. S6B). In addition, localization of mitochondria, which are carried by KHC, is largely unaffected, and its transport is still maintained at a signifi-

Figure 3. Physical interaction of UNC-51, UNC-76, and KHC. (A) Myc-tagged UNC-51 (full-length) and HA-tagged UNC-76 (truncation mutants) were coexpressed in HEK293T cells as indicated. Cell lysates were immunoprecipitated by anti-HA followed by immunoblot with anti-myc. (*) Nonspecific band (22 kDa) detected by anti-HA antibody. (B) UNC-51 binds UNC-76 in vitro. GST alone or GST fused with full-length UNC-76 was produced in *E. coli*, purified on Glutathione-Sepharose beads, and incubated with myc-tagged UNC-51 C'-terminal domain (amino acids 557–855) produced by in vitro translation (IVT). Proteins that bound to the beads were eluted and analyzed by immunoblot using anti-myc. (C) Schematic representation of the domains involved in UNC-51–UNC-76 binding. Black bars show deletion constructs that bind the other in coimmunoprecipitation assays. Constructs shown in gray did not bind. Binding of all deletion constructs except for UNC-76 (118–340 amino acids) with UNC-51 was confirmed by GST pull-down assay (data not shown). The UNC-76 and UNC-51 functional domains are indicated within each protein. (D) UNC-51 forms a complex with KHC via UNC-76. HEK293T cell extracts containing heterologously expressed UNC-51 (full-length), UNC-76 (full-length), and KHC (full-length), as indicated, were analyzed by immunoprecipitation with anti-HA followed by immunoblot with the indicated antibodies.



cant level in *unc-51* mutants (Supplemental Fig. S3C,D; Supplemental Movie S1). Although these data do not rule out the possibility that kinesin activity or cytoskeletal function is impaired in *unc-51* mutants, we investigated the additional possibility of motor–cargo uncoupling, and analyzed the detailed localization of cargoes and motor complexes in *unc-51* mutants.

Notably, SV aggregates were nearly completely segregated from UNC-76-positive domains in *unc-51* mutants, whereas only diffuse patterns of staining with SV and UNC-76 were observed for wild type (Fig. 4A), consistent with previous studies (Gindhart et al. 2003). Quantitative analysis showed that 62.5% of all puncta seen in *unc-51* mutants were Syt-1 single-positive, 35% were UNC-76 single-positive, and only 2.5% were Syt-1/UNC-76 double-positive (Fig. 4A, graph). Next, UNC-76 localization was compared with that of KHC within *unc-51* mutant axons. Fifty-six percent of puncta were UNC-76/KHC double-positive, 7% were UNC-76 single-positive, and 37% were KHC single-positive (Fig. 4B, graph), indicating that a large fraction of UNC-76-positive puncta were also positive for KHC, suggesting that *unc-51* activity is dispensable for the interaction of UNC-76 with KHC. An analysis of CSP-positive and KHC-positive puncta in *unc-51* mutants revealed that 18% of puncta were CSP/KHC double-positive, 37% were CSP single-positive, and 45% were KHC single-positive (Fig. 4C, graph). Taken together, these data raise the possibility that SVs are dissociated from motor complexes in *unc-51* mutants.

To provide a detailed view of the relationship between SV and UNC-76 in normal transport, high-resolution images of CSP and UNC-76 double-staining were analyzed in wild-type SGNs in comparison with *unc-51* mutant SGNs (Fig. 4D). Both CSP and UNC-76 showed widespread distributions in wild-type SGNs. Among total area positive for either CSP or UNC-76, 18% was CSP/UNC-76 double-positive, 11% was UNC-76 single-positive, and 71% was CSP single-positive in wild type. In *unc-51* mutants, the CSP/UNC-76 double-positive area was significantly less (4%) and the UNC-76 single-positive area was greater (23%) than in wild type, whereas the CSP single-positive area was similar to that in wild type (73%) (Fig. 4D, graph), which was consistent with the Syt-1/UNC-76 double-staining results (Fig. 4A). The data suggest that ~20% of SVs are carried by UNC-76-containing motor machinery in wild type, and that *unc-51* mediates the coupling of this fraction of SVs with UNC-76-containing motor complexes.

These data, together with the previous finding that *unc-76* mutants have a SV aggregation defect (Gindhart et al. 2003), led us to hypothesize that UNC-76 mediates the coupling of SVs and KHC motors. Immunohistochemical analysis revealed a disorganized localization of SVs and KHC in *unc-76* mutants (Supplemental Fig. S7), similar to that observed in *unc-51* mutants. Therefore, the data suggest that UNC-76 and UNC-51 cooperatively function in axonal transport likely through the regulation of motor–cargo coupling.

Phosphorylation of UNC-76 Ser¹⁴³ is critical for axonal transport

To provide molecular insight into how UNC-51 and UNC-76 cooperatively control motor–cargo assembly, we investigated whether UNC-51 kinase phosphorylates UNC-76, because the transgene rescue experiments demonstrated the importance of UNC-51 kinase activity in axonal transport in vivo (Fig. 1D). In an in vitro kinase assay using [γ -³²P]-ATP, UNC-76 incorporated ³²P in an UNC-51 kinase-dependent manner (Fig. 5A). In the heterologous expression system in HEK293T cells, UNC-76 showed a mobility shift in the presence of wild-type UNC-51, which was abolished by phosphatase treatment (Fig. 5B). In contrast, kinase-deficient UNC-51/K38A failed to produce a mobility shift of UNC-76 (Fig. 5C).

To identify specific phosphorylated residue(s) within UNC-76, we introduced a series of Ala mutations into the five Ser/Thr residues that are evolutionarily conserved among *C. elegans*, *Drosophila*, and rat UNC-76 (Bloom and Horvitz 1997; Kuroda et al. 1999; Gindhart et al. 2003). When expressed in HEK293T cells together with UNC-51 kinase, only the UNC-76/S143A mutation failed to produce the mobility shift (Fig. 5C), indicating that Ser¹⁴³ is the site of phosphorylation. Mass spectrometric analysis of UNC-76 proteins phosphorylated by UNC-51 in HEK293T cells also confirmed Ser¹⁴³ as a phosphorylation site (Supplemental Fig. S8). Ser¹⁴³ phosphorylation was further verified in vivo using an antibody raised against a phospho-Ser¹⁴³-containing UNC-76 peptide. Phospho-UNC-76 was detected in extracts from wild-type larvae but not from *unc-51* mutants (Fig. 5D). To provide in vivo evidence that UNC-76 Ser¹⁴³ phosphorylation is necessary for normal axonal transport, we introduced wild-type UNC-76, a phosphomimetic UNC-76/S143D or a phosphodeficient UNC-76/S143A transgene into the *unc-76* mutant background, and tested whether each transgene could rescue the axonal transport defect. UNC-76/wt and UNC-76/S143D rescued the SV and KHC aggregation phenotypes in SGNs, but UNC-76/S143A failed to rescue the defects (Fig. 5E). In accordance with these results, the amount of total SVs found in NMJ synapses (segment A2, muscle 6/7) of the rescued larvae was significantly greater than in nonrescued larvae (Supplemental Fig. S9). In the rescued larvae (*unc-76*^{-/-}; *elav* > *unc-76*^{WT} and *unc-76*^{-/-}; *elav* > *unc-76*^{SD}), the numbers of synaptic boutons, size of the bouton area, and total amount of CSP staining in NMJs were elevated as compared with nonrescued larvae (*unc-76*^{-/-}; *elav* > *unc-76*^{SA}), suggesting that the UNC-76/wt or UNC-76/S143D transgenes rescued the SV transport defect. Collectively, these data demonstrate a critical role for UNC-51-mediated phosphorylation of UNC-76 Ser¹⁴³ in controlling axonal transport.

Phosphorylation-dependent interaction of UNC-76 and Syt-1

Because loss of UNC-76 phosphorylation led to defective axonal transport (Fig. 5E) and loss of *unc-76* resulted in

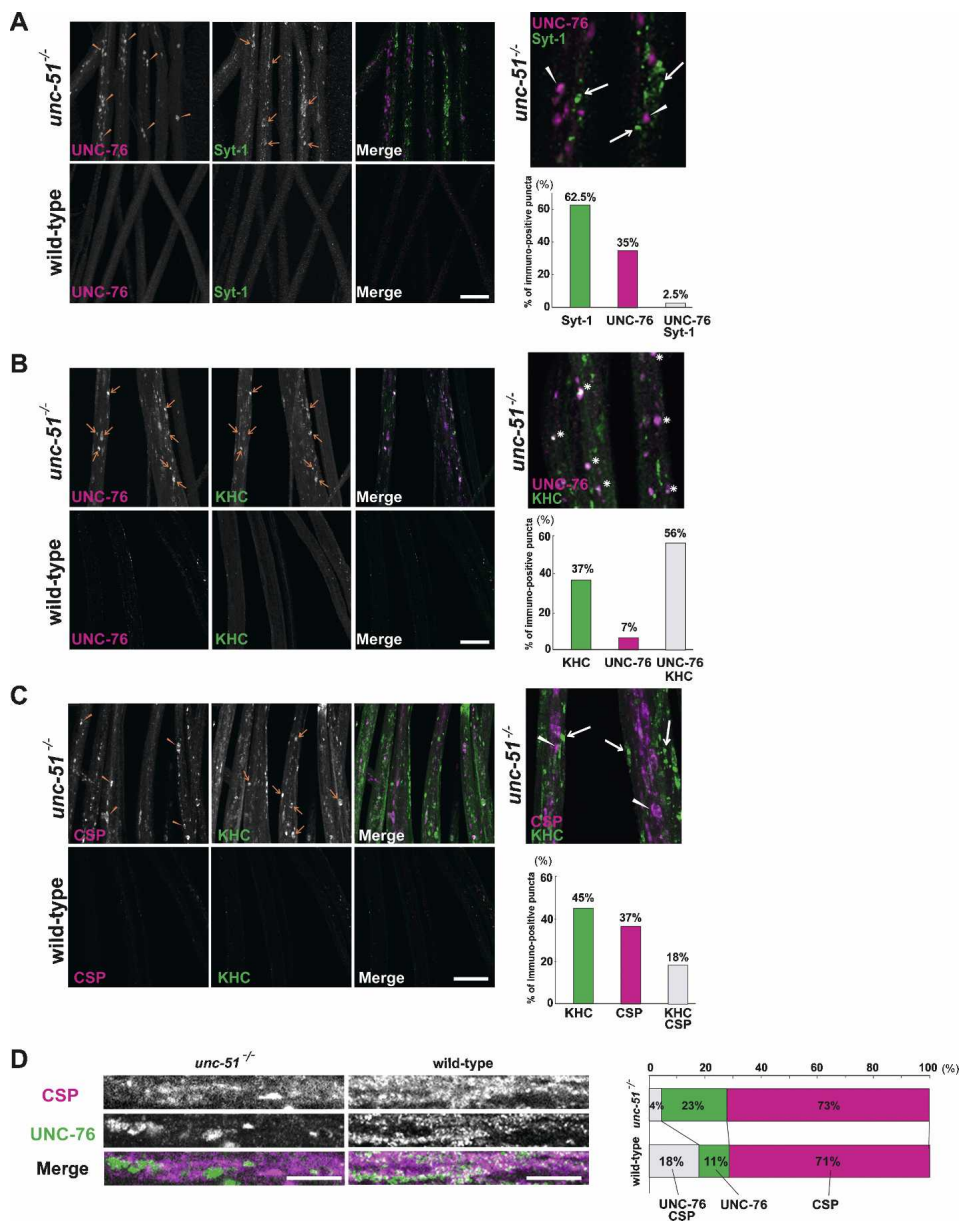


Figure 4. Disorganized localization of SV and motor complexes in *unc-51* mutants. (A) SGNs of *unc-51* mutants (*unc-51³/unc-51²⁵*) or wild-type third instar larvae immunostained with anti-UNC-76 (red) and anti-Syt-1 (green). Red arrows and arrowheads point to aberrant localization of the indicated proteins. The right panel shows enlarged image (arrowheads, UNC-76; arrows, Syt-1). The numbers of puncta positive for UNC-76 and/or Syt-1 in *unc-51* mutant SGNs were scored and the percentages of single-positive or double-positive puncta are shown in the graph. SGNs are oriented from the proximal side (top) toward the distal (bottom). (B) SGNs of *unc-51* mutants or wild-type larvae immunostained with anti-UNC-76 (red) and anti-KHC (green). Red arrows point to aberrant localization of the indicated proteins. The right panel shows enlarged image (asterisks, KHC/UNC-76 double-positive aggregates). The numbers of puncta positive for UNC-76 and/or KHC in *unc-51* mutant SGNs were scored and the percentages of single-positive or double-positive puncta are shown (graph). (C) SGNs of *unc-51* mutants or wild-type larvae immunostained with anti-CSP (red) and anti-KHC (green). Red arrows and arrowheads point to aberrant localization of the indicated proteins. Right panel shows enlarged image (arrowheads, CSP; arrows, KHC). (Graph) The numbers of puncta positive for CSP and/or KHC in *unc-51* mutant SGNs were scored and the percentages of single-positive or double-positive puncta are shown. (D) SGNs of *unc-51* mutant or wild-type larvae immunostained with anti-CSP (red) and anti-UNC-76 (green) and observed with confocal microscopy (with 100× objective; single optical section taken at 0.7-μm interval). SGNs are oriented from the proximal side (left) toward the distal (right). Areas positive for CSP, UNC-76 or both signals were calculated based on the confocal data using an image analysis program, and schematically represented on the graph. Bars, 10 μm.

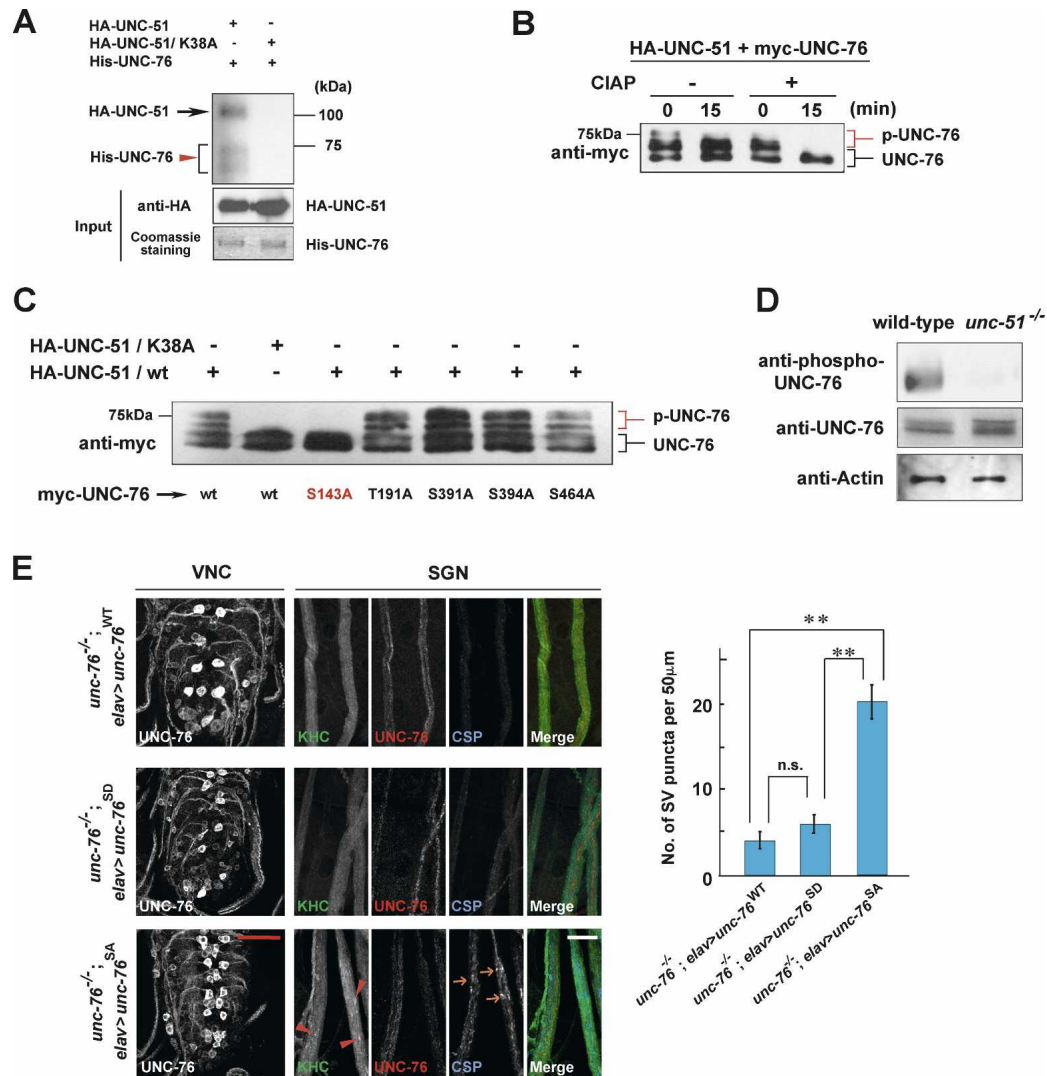


Figure 5. Phosphorylation of UNC-76 Ser¹⁴³ by UNC-51 is necessary for axonal transport. (A) In vitro phosphorylation of UNC-76 by UNC-51 kinase. HA-tagged UNC-51 or UNC-51/K38A expressed in HEK293T cells was immunoprecipitated and incubated with His-UNC-76 in the presence of Mg²⁺ and [γ -³²P]-ATP. Phosphoproteins were analyzed by autoradiograph. Black arrow indicates UNC-51 autophosphorylation. Red arrowhead indicates UNC-76 phosphorylation. (B) Myc-tagged UNC-76 and HA-tagged UNC-51 were coexpressed in HEK293T cells. Cell lysates were incubated for an indicated period of time with (+) or without (-) alkaline phosphatase (CIAP) and analyzed by immunoblot using anti-myc. Red bracket indicates mobility shifts of UNC-76. Black bracket indicates nonshifted UNC-76. (C) Myc-tagged wild type and Ser/Thr → Ala mutant UNC-76 were expressed in HEK293T cells with UNC-51 or UNC-51/K38A. Cell lysates were analyzed by immunoblot using anti-myc. Red bracket indicates mobility shifts of UNC-76. (D) Extracts from wild-type and *unc-51* mutant larvae were analyzed by immunoblot using an anti-phospho-UNC-76 antibody. Anti-actin and anti-UNC-76 were used as loading controls. (E) Genetic rescue of axonal transport defect in *unc-76* mutants by *unc-76* transgene. CSP-positive aggregation (arrows) and KHC aggregation (arrowheads) in *unc-76* mutants were rescued by *unc-76*^{WT} (top) or *unc-76*^{S143D} (middle), but not by *unc-76*^{S143D} transgene (bottom). Transgene expression was driven by *elav*. *unc-76*^{DR1107} hemizygous males were used as *unc-76*-null mutants. Third instar larvae for each genotype were stained with anti-KHC (green), anti-UNC-76 (red), and anti-CSP (blue). Note the equivalent expression levels of UNC-76 transgenes in VNC and SGN. (**) Statistical significance ($P < 0.01$, Student *t* test). (n.s.) Not significant ($P = 0.18$). Bars: red, 50 μ m; white, 20 μ m.

disorganized motor-cargo distribution (Supplemental Fig. S7), we hypothesized that the phosphorylation of UNC-76 by UNC-51 may regulate the affinity of UNC-76 to SV cargoes. Although FEZ1, a rat homolog of UNC-76, bound Syt-1 in a yeast two-hybrid screen (Bloom and Horvitz 1997), whether they physically interact was not successfully confirmed. Indeed, we did not detect an in-

teraction between Syt-1 and UNC-76 in coimmunoprecipitation assays using the HEK293T expression system (Fig. 6A). However, UNC-76 copurified with Syt-1 in the presence of UNC-51, but not in the presence of kinase-deficient UNC-51/K38A (Fig. 6A). The association between UNC-76 and Syt-1 was abolished by phosphatase treatment (Fig. 6B), indicating that their interaction is

phosphorylation-dependent. Although Syt-1 often binds its partners in a Ca^{2+} -dependent manner (Südhof 2004), the interaction between Syt-1 and UNC-76 was Ca^{2+} -independent (Fig. 6C). In addition, the phosphomimetic

UNC-76/S143D associated with Syt-1, whereas the phosphodeficient UNC-76/S143A did not (Fig. 6A).

A direct interaction between UNC-76 and Syt-1 was further confirmed by Förster resonance energy transfer

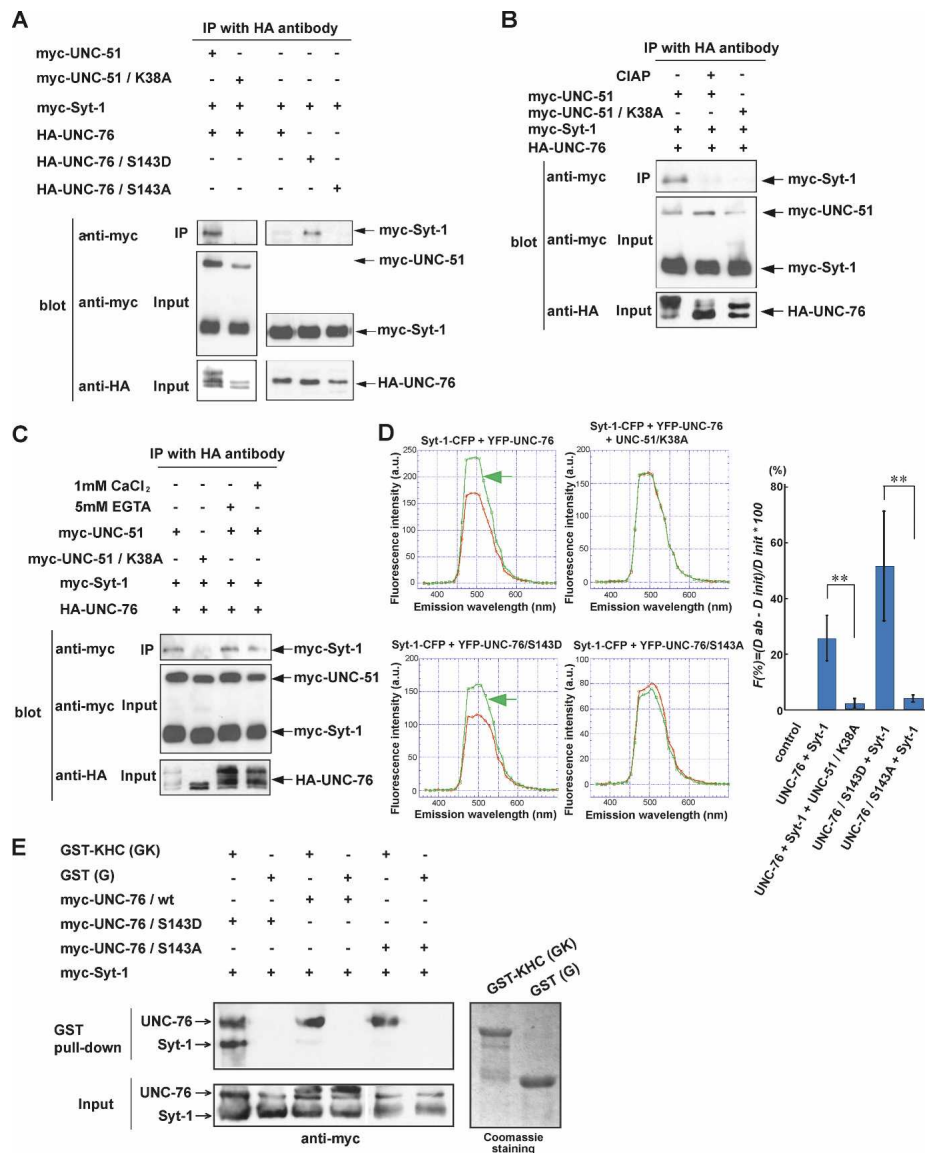


Figure 6. UNC-51 regulates the affinity between UNC-76 and Syt-1. (A) UNC-51-mediated association of Syt-1 and UNC-76. Myc- or HA-tagged UNC-51 (full-length), UNC-76 (full-length), and Syt-1 (full-length) were coexpressed in HEK293T cells as indicated. Cell lysates were immunoprecipitated by anti-HA followed by immunoblot with anti-myc. (B) Phosphorylation-dependent association of Syt-1 and UNC-76. HA-UNC-76, myc-Syt-1, and myc-UNC-51 or UNC-51/K38A were expressed in HEK293T cells as indicated. Cell lysates were immunoprecipitated with anti-HA. The immunocomplexes were incubated in the presence (+) or absence (-) of alkaline phosphatase (CIAP) and analyzed by immunoblot using anti-myc. (C) Syt-1-UNC-76 interaction does not require Ca^{2+} . HA-UNC-76, myc-Syt-1, and myc-UNC-51 or UNC-51/K38A were expressed in HEK293T cells as indicated. Cell lysates were immunoprecipitated with anti-HA. The immune complexes were incubated in the presence of EGTA or CaCl_2 and analyzed by immunoblot using anti-myc. (D) Syt-1-UNC-76 interaction detected by FRET. COS7 cells were transfected with Syt-1-CFP, YFP-UNC-76, YFP-UNC-76/S143D, YFP-UNC-76/S143A, or UNC-51/K38A in combination as indicated. For each combination, initial (red) and fluorescence after acceptor photobleaching spectra (green) were plotted for a range of wavelengths indicated. Increase in donor fluorescence after acceptor bleaching indicates FRET (green arrows). Quantification of FRET (graph). (***) Statistical significance ($P < 0.01$). (E) KHC/UNC-76/Syt-1 complex formation. GST alone (G) and GST fused with KHC (amino acids 675–975) (GK) were produced in *E. coli*, purified on Glutathione-Sepharose beads, and incubated with myc-UNC-76 and myc-Syt-1 expressed in HEK293T cells. Proteins that bound to the beads were eluted and analyzed by immunoblot using anti-myc.

(FRET) analysis in cultured cells. Coexpression of Syt-1-CFP and YFP-UNC-76 in COS7 cells gave rise to FRET between the two proteins (Fig. 6D), presumably via the phosphorylation of UNC-76 by endogenous UNC-51 kinase. Indeed, the FRET signal was attenuated by kinase-deficient UNC-51/K38A (Fig. 6D), suggesting a specific role of UNC-51 kinase activity in the Syt-1-UNC-76 interaction. In addition, Syt-1-CFP and the phosphomimetic YFP-UNC-76/S143D produced FRET, whereas Syt-1-CFP and the phosphodeficient YFP-UNC-76/S143A did not (Fig. 6D), further confirming the role of Ser¹⁴³ phosphorylation in the Syt-1-UNC-76 interaction. Thus, the data demonstrate that the adaptor protein UNC-76 directly interacts with Syt-1 on the SVs, and that this interaction is regulated by UNC-51 kinase activity.

To further address whether KHC/UNC-76-containing motor complex could interact with Syt-1 in a phosphorylation-dependent manner, we carried out a GST pull-down assay (Fig. 6E). GST-fused KHC, which bound UNC-76 (Gindhart et al. 2003), interacted with Syt-1 in the presence of UNC-76/S143D, but not in the presence of UNC-76/S143A or unphosphorylated UNC-76/wt. Consistent with *in vivo* observation (Fig. 4B), UNC-76 bound KHC regardless of the phosphorylation status at Ser¹⁴³ (Fig. 6E; Supplemental Fig. S10). Taken together, association of UNC-76 with Syt-1, but not with KHC, is mediated by phosphorylation of UNC-76 Ser¹⁴³ by UNC-51 kinase.

Discussion

Nature of defective axonal transport in unc-51 mutants

This study demonstrates that loss of *unc-51* function affects the transport of several axonal cargoes, including SV and mitochondria. In *unc-51* mutants, SV transport is severely attenuated and many SV aggregates are found along the larval SGN axons. SV aggregation in *unc-51* mutants is similar to that observed in *Khc* mutants (Hurd and Saxton 1996). However, unlike *Khc* mutants, SV aggregates in *unc-51* mutants do not contain mitochondria, suggesting that the aggregated SVs in *unc-51* mutants do not cause overall "steric hindrance," in which the impaired cargo interferes with the transport of other cargoes as a secondary effect. In *unc-51* mutants, Rab5-positive membranes also exhibited a pattern of aggregation different from that for SVs, supporting the idea that loss of *unc-51* results in defective axonal transport in a membrane type-dependent manner. This view is further supported by a recent analysis of *unc-51* mutants in *C. elegans* that showed that only a subset of cargoes are selectively mislocalized, whereas a majority of other cargoes are not affected (Ogura and Goshima 2006).

SVs are one of the most severely affected axonal cargoes in *unc-51* mutants. Two anterograde motors, kinesin-1 and kinesin-3, have been implicated in SV transport in *Drosophila*. A recent study addressed an essential role of *unc-104* (*imac*, kinesin-3) in SV transport (Pack-

Chung et al. 2007). Virtually all SVs fail to enter axons and accumulate in neuronal cell bodies during the embryonic period. In contrast, mutations in *Khc*, a catalytic component of kinesin-1, and also mutations in *Klc*, an accessory component of kinesin-1, cause SV accumulations within axons of larval SGNs (Hurd and Saxton 1996; Gindhart et al. 2003). These studies suggest that, although kinesin-3 is primarily responsible for SV transport, kinesin-1 plays a role in SV transport in a manner distinct from that for kinesin-3, or the two motors may have complementary roles in SV transport at the larval stage. The *unc-51* mutant phenotypes, as well as the biochemical evidence that UNC-51 forms a complex with UNC-76/KHC, are most consistent with the idea that UNC-51 functions in SV transport through a kinesin-1-dependent pathway.

In *unc-51* mutants, SVs accumulate within axons at sites distant from cell bodies, suggesting that SVs could partially transport along axons in the absence of *unc-51*. It is possible that maternally deposited *unc-51* contributes to partial transport of SVs into axons, as suggested for defective SV transport in *Khc* mutants (Hurd and Saxton 1996). It is also possible that there are specific subcellular locations (e.g., axon hillock) or earlier developmental periods where SV transport does not require *unc-51* activity. The axonal SV accumulation in *unc-51* mutants could be a result of spatially distinct requirement of *unc-51* activity for maintaining SV-motor integrity during transport. In addition, as we discussed, kinesin-3 likely contributes to SV transport in *unc-51* mutants, resulting in translocation of a subset of SVs into axons and to synapses. SVs that are localized to *unc-51* mutant NMJs may reflect a subpopulation of those that were carried by kinesin-3 and did not need *unc-51* activity for their transport. In summary, the cooperative action of multiple pathways, including *unc-51*, *unc-76*, kinesin-1 and kinesin-3, may be necessary for complete SV transport.

Phosphorylation-mediated motor-cargo assembly

Previous *in vitro* studies that addressed a role of phosphorylation in regulating organelle motility have remained unclear and controversial. A series of kinases, including PKA, PKC, and PKG, were shown to have no effect on kinesin-dependent axonal transport (Bloom et al. 1993), whereas phosphorylation of kinesin by PKA was proposed to inhibit fast axonal transport and kinesin binding to membrane organelles (Sato-Yoshitake et al. 1992; Okada et al. 1995). Glycogen synthase kinase 3 β (GSK3 β) phosphorylates KLC and kinesin-based motility is inhibited by perfusion of active GSK3 β into squid axons (Morfini et al. 2002). An inhibitory effect of CaMKII in disrupting KIF17-Mint1 association *in vitro* has recently been reported (Guillaud et al. 2008). However, it was not until recently that the physiological role of phosphorylation in axonal transport was addressed *in vivo* (Horiuchi et al. 2007), in which JNK-mediated phosphorylation inhibits the kinesin-1-JIP1 adaptor interaction.

Our study has revealed a critical role of UNC-76 phosphorylation during axonal transport, which is likely elicited at the motor–cargo interface. Several lines of evidence support this notion. First, *unc-51* genetically interacts with the kinesin-1 adaptor *unc-76* in axonal transport *in vivo*. Second, biochemical experiments show that the association of UNC-76 and Syt-1 is mediated by UNC-51-dependent phosphorylation of UNC-76. Third, FRET analysis confirms the direct association between UNC-76 and Syt-1 in cells, which is attenuated by inhibiting UNC-51 kinase activity. Finally, the SV transport defects of *unc-76* mutants are rescued *in vivo* by phosphomimetic UNC-76, but not by phosphodeficient UNC-76.

Based on these findings, we propose a model in which adaptor phosphorylation is a key regulatory step that maintains motor–cargo association within axons and leads to efficient SV transport (Fig. 7). Upon phosphorylation by UNC-51 kinase, UNC-76 displays an increased affinity to SV membrane proteins such as Syt-1. Attenuation of UNC-51 kinase activity would reduce the affinity of UNC-76 for SV membrane proteins and cause the

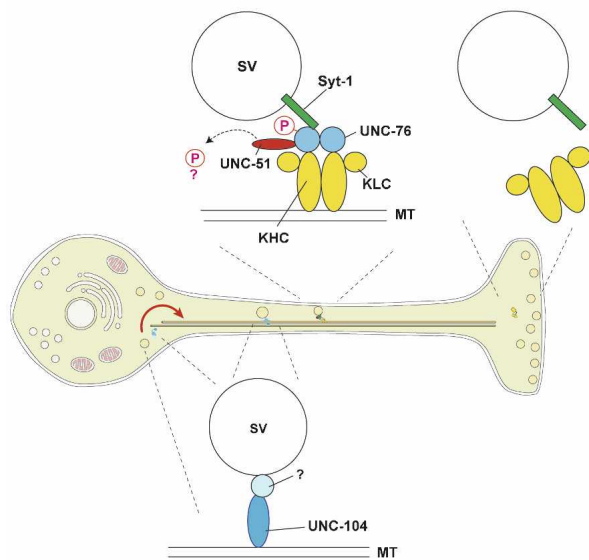
dissociation of SV cargoes from the motor complexes. In our model, motor–cargo affinity could also be reduced by dephosphorylation of UNC-76, although such regulatory factor is yet to be identified. Attenuation of UNC-51 activity or activation of phosphatase activity could explain the mechanism of SV cargo detachment from the kinesin motors. Additional work is needed to determine how UNC-51 kinase activity is spatially and temporally controlled to regulate axonal transport. It is notable that both UNC-51 and UNC-76 are undetectable at NMJ of the wild-type third instar larvae (Supplemental Fig. S11), suggesting a spatial control of motor–cargo dissociation at the axonal termini.

The proposed mechanism can explain the transport of a subset of SVs. Only ~20% of SVs appear to colocalize with UNC-76 in wild-type SGNs (Fig. 4D), suggesting that an additional motor/adaptor system, such as kinesin-3, is responsible for carrying the rest of the SVs at the larval stage, as discussed earlier. Indeed, a subpopulation of SVs successfully reaches the synapses in *unc-51* mutant NMJs, although these synaptic boutons are smaller in size and fewer in number (Supplemental Fig. S2). It is also likely that UNC-51/UNC-76/kinesin-1 activity is dispensable for loading SVs onto the motor complexes at cell bodies, because SV aggregates are found within axons and distant from cell bodies in these mutants. Thus, the UNC-51/UNC-76/kinesin-1 complex seems important for maintaining motor–cargo association within axons rather than being responsible for initial cargo loading. Alternatively, maternally deposited *unc-51* or *Khc* may contribute to partial transport of SVs into axons, as discussed earlier, and the potential role of UNC-51/UNC-76/kinesin-1 complex in initial cargo loading may be masked in our analysis of *unc-51* mutants.

Although our study clearly demonstrates that phosphorylation of UNC-76 by UNC-51 kinase is critical for SV transport, the phosphomimetic UNC-76 transgene failed to rescue defective SV transport in *unc-51* mutants (data not shown). This implies that phosphorylation of UNC-76 is not sufficient for SV transport, and suggests that additional targets of UNC-51 phosphorylation are necessary for proper SV transport. Both KHC and KLC are phosphoproteins (Hollenbeck 1993; Morfini et al. 2002), and *unc-51* interacts genetically with *Klc*. Therefore, additional transport components, including KHC and KLC, need to be tested as candidate substrates for UNC-51 kinase in order to understand the whole picture of *unc-51*-mediated axonal transport machinery.

It is unclear how loss of *unc-51* results in aggregation of the kinesin motor complex. Biophysical studies show that cargo binding to the kinesin tail domain is required to unfold kinesin molecules and to activate their motor function on MTs (Coy et al. 1999; Friedman and Vale 1999; Hackney and Stock 2000), suggesting that a failure of motor–cargo assembly could cause stalling and aggregation of kinesin motors. With respect to the kinesin motor activation, a recent report has addressed a novel role for UNC-76/FEZ1 in kinesin motor unfolding and thus activation (Blasius et al. 2007). In this model, two

Kinesin-1-dependent transport



Kinesin-3-dependent transport

Figure 7. Schematic model for UNC-51 kinase-mediated motor–cargo assembly. Our results suggest a model in which UNC-51 kinase functions in axonal transport via the kinesin-1-dependent pathway. When phosphorylated by UNC-51 kinase, UNC-76, a KHC adaptor and a potential activator of kinesin-1, displays an increased affinity to SV membrane proteins such as Syt-1. UNC-51 likely phosphorylates additional substrates that are essential for axonal transport (dashed arrow). Loss or attenuation of UNC-51 kinase activity would result in a lower affinity of UNC-76 to SV membrane proteins and dissociation of SV cargoes from the motor complexes, as might be the case at NMJ. Kinesin-3 (*imac*/UNC-104) is also responsible for SV transport in a large fraction and is important for carrying SVs from neuronal soma to axons and synapses (red arrow).

scaffolding/adaptor proteins, JIP1 and UNC-76/FEZ1, induce a step-wise conformational change in kinesin-1, leading to its full activation as a motor *in vitro*. In good agreement with this model, loss of *unc-76* results in disorganized localization of SVs and KHC *in vivo* (Supplemental Fig. S7). Taken together with our finding that the phosphomimetic UNC-76 is capable of rescuing axonal transport defects in *unc-76* mutants, it is possible that UNC-76/FEZ1 not only serves as a motor-cargo linker, but also functions as a kinesin-1 activator in a phosphorylation-dependent manner. Thus, this phosphorylation-dependent regulation of adaptors may address an additional mechanism for controlling kinesin-1 activity that is essential for axonal transport.

Although the *unc-51* and *unc-76* pathways could cooperatively activate kinesin-1 activity, it is unlikely that loss of *unc-51* leads to complete loss of *Khc* activity. In *unc-51* mutants, mitochondrial transport is partially attenuated, but the majority of mitochondria are still transported, suggesting that the overall activity of KHC, a major motor for mitochondrial transport (Stowers et al. 2002), is preserved. This view is supported by our immunohistochemical evidence, which shows that a subpopulation of KHC is present in aggregates, whereas the rest of KHC was distributed throughout the axons. This suggests that a part of KHC activity may be unaffected in *unc-51* mutants, and that the UNC-76-independent population of KHC is functionally active and participate in the transport of other cargoes. Although UNC-51 forms a complex with KHC via UNC-76 and KHC distribution is altered in *unc-51* mutants, which strongly suggests a functional interaction between UNC-51 and KHC, it is possible that UNC-51 regulation of kinesin-1 activity is mediated through UNC-76 or an additional factor such as KLC, and the effect of UNC-51 on the KHC motor may be indirect. In this regard, it is suggestive that *unc-76* and *unc-51* show a clear genetic interaction, whereas *Khc* and *unc-51* do not exhibit an apparent genetic interaction.

Implication of unc-51-mediated regulatory process in additional biological contexts

Our model of phosphorylation-dependent regulation of motor-cargo assembly could be extended to include additional adaptors or cargo vesicles. UNC-14, a protein that interacts with UNC-51 (Ogura et al. 1997), has recently been reported to play a role in kinesin-1-dependent axonal transport in *C. elegans* (Sakamoto et al. 2005). UNC-14 might serve as an adaptor for the kinesin motor complex to regulate motor-cargo affinity in an UNC-51-dependent manner. In addition, *unc-51* mutations also result in aggregation of vesicles positive for UNC-5, a Netrin/UNC-6 receptor (Ogura and Goshima 2006). Again, affinity between the UNC-5-positive vesicles and their respective motor complexes might be regulated by UNC-51-dependent phosphorylation.

Previous studies in worms and mice (Ogura et al. 1994; Tomoda et al. 2004), as well as this study, addressed a role of *unc-51* in axon formation. It remains to be studied

whether our model could be extended to explain the regulation of membrane components necessary for axon formation, in which the assembly of axonal membranes with the corresponding motors may be mediated via *unc-51*-dependent phosphorylation.

Recent studies identified *unc-51* as a homolog of *atg1*, which plays a role in autophagy (Scott et al. 2004, 2007), a catabolic cellular process responsible for bulk degradation of proteins and organelles, particularly when cells are under nutrient-deprived conditions (Klionsky and Ohsumi 1999). Disruption of the autophagy genes *atg5* or *atg7* in mouse brains results in neuronal cell death, which accompanies intracellular accumulation of ubiquitin-positive aggregates (Hara et al. 2006; Komatsu et al. 2006). We observed neither ubiquitin-positive aggregates nor symptoms of cellular death in *unc-51* mutant SGNs (data not shown), suggesting that the role of *unc-51/atg1* in axonal transport is distinct from its role in autophagy, which is induced under nutrient-deficient conditions (Scott et al. 2004). Although autophagy critically depends on intracellular vesicle transport (Klionsky and Ohsumi 1999), and UNC-51 kinase activity seems to be required for autophagy induction (Scott et al. 2007), a link between axonal transport and autophagy remains to be studied.

In conclusion, our study identifies a novel regulatory step for axonal transport that depends on the UNC-51 kinase-mediated phosphorylation of a kinesin adaptor. Further studies on the regulation of *unc-51* activity will provide us with a better understanding of axonal transport, as well as dynamic neuronal control of synaptic development and plasticity.

Materials and methods

Drosophila strains and maintenance

Fly strains were maintained on standard medium at 25°C. The following mutants and transgenic fly strains were used: *OK6-Gal4* (gift from Christoph Schuster), *UAS-mito::GFP* (gift from Bill Saxton; Horiuchi et al. 2005), *Syd^{1D1}* and *Syd^{2H2A}* (gift from Larry Goldstein), *UAS-LAMP1::GFP* (gift from Helmut Krämer; Pulipparacharuvil et al. 2005), *Dhc64C^{KG08838}*, *Dhc64C⁴⁻¹⁹*, *elav^{c155}-Gal4*, *Khc⁸*, *Klc^{8ex94}*, *unc-76^{1(1)G0360}*, *unc-76^{Df(1)107}*, *Aplip1^{ek4}*, *Aplip1^{Df(3L)Fpa2}*, *unc-104^{d11204}*, *Lis-1^{K13209}*, *UAS-Syt-1::eGFP*, *UAS-Rab5::YFP* (Bloomington *Drosophila* Stock Center; Zhang et al., 2007; YFP tag at the N' terminus of Rab5), *EP(3)3348* (Szeged *Drosophila* Stock Center), *Df(3L)ED4486* (European *Drosophila* Stock Center). Fly lines carrying transgenes (*UAS-unc-51*, *UAS-unc-51^{K38A}*, *UAS-Venus::unc-51*, *UAS-unc-76*, *UAS-unc-76^{S143D}*, *UAS-unc-76^{S143A}*) were generated by Genetic Services, Inc., or by Rainbow Transgenic Flies, Inc.

Plasmid construction

Full-length UNC-51 (LD18893), UNC-76 (LD08195), and KHC (SD02406) cDNAs were obtained from DGRC (*Drosophila* Genetic Resource Center, Kyoto). To obtain the full-length *Syt-1* cDNA, RT-PCR was performed on mRNA purified from wild-type third instar larval brain. The coding regions of these genes were inserted into the *Sall*/*NotI* sites of *pRK5-HA/myc* for expression in mammalian cells, *pGEX4T-2* for GST fusion protein

expression in *Escherichia coli*, pET-28c(+) for 6xHis tag protein expression in *E. coli*, or into the EcoRI/NotI sites of pUAST for expression in *Drosophila*. Deletion constructs of UNC-51 and UNC-76 were amplified by PCR. Single amino acid point mutations were introduced into UNC-51 and UNC-76 by site-directed mutagenesis. Syt-1 and UNC-76 were fused in-frame with Cerulean and Venus, blue (CFP) and yellow (YFP) variants of green fluorescent protein (GFP), respectively, with a linker sequence of six glycine residues at the fusion site, and inserted into the Sall/NotI sites of pRK5.

Larval tissue staining

Larval tissue preparation and staining were done as described in Kurusu et al. (2002). The primary antibodies used were rabbit anti-Syt-1 (1:1,000; gift from Troy Littleton), guinea pig anti-UNC-76 (1:100), guinea pig anti-UNC-51 (1:100), mouse anti-CSP (1:10; Developmental Studies Hybridoma Bank [DSHB]), mouse anti-FasII (1:10; DSHB), FITC-conjugated HRP (1:100; Jackson ImmunoResearch), rabbit anti-KHC (1:200; Cytoskeleton, Inc.), and mouse anti-Futsch (MAP1B-like; 22C10) (1:5; DSHB). The secondary antibodies used were Alexa 543-conjugated goat anti-rabbit, Alexa 488-conjugated goat anti-rabbit, Alexa 543-conjugated goat anti-guinea pig, and Alexa 633-conjugated goat anti-mouse (1:500; Molecular Probes). To quantify the number of aggregates for CSP, Syt-1, KHC, or UNC-76, background levels were subtracted from each image file by applying a threshold (scaling factor 4) and the particle numbers scored using ImageJ software (NIH). In situ analysis of *unc-51* mRNA expression was done as described in Hauptmann and Gerster (2000), using full-length *Drosophila unc-51* cDNA.

Time-lapse video microscopy

Wild-type or *unc-51* mutant wandering third instar larvae carrying both UAS-*mito::GFP* and the motor neuron driver *OK6-Gal4*, or those carrying both UAS-*Syt-1::eGFP* and *OK6-Gal4* were dissected quickly (<2 min) in Schneider culture medium and the exposed nerves were mounted on a coverslip. Time-lapse imaging was performed with a Zeiss LSM 510 using 100 \times objectives [1 fps for *mito::GFP*, and 5 fps [200-msec interval between frames] for *Syt-1::eGFP*]. To increase the signal, the pinhole was opened to two Airy units. In the movies, the SGNs are oriented with anterior to the left and posterior to the right. The *Syt-1::eGFP* movies play at two times real time, and the *mito::GFP* movies play at five times real time. *Mito::GFP*-positive or *Syt-1::eGFP*-positive packets were individually tracked for every frame, and their average transport speeds (distance traveled by each packet/[1 sec or 200 msec \times frame numbers]) were calculated by Image Pro Plus software (Media Cybernetics, Inc.).

Antibody generation

To generate the anti-UNC-51 antibody, the C'-terminal domain of UNC-51 (amino acids 557–855) fused to GST was produced in *E. coli*, purified on Glutathione-Sepharose 4B beads, and injected into guinea pigs (MBL). The resulting antiserum was adsorbed against GST and then affinity-purified using a column containing GST-UNC-51 (amino acids 557–855). To generate a phosphospecific UNC-76 antibody, an UNC-76 peptide that contained phospho-Ser¹⁴³ (TETFGG[*p*S]LEDLVN) was synthesized, HPLC-purified, and conjugated to KLH. Eggs laid by two immunized chicks were pooled and the whole IgY fractions were purified by Aves Laboratories. This antibody detects a band of an apparent molecular mass that is greater than the

expected MW of UNC-76, presumably due to modification of UNC-76 in vivo, via post-translational modification such as phosphorylation.

Coimmunoprecipitation

Coimmunoprecipitation assays in heterologous expression systems were done as described in Tomoda et al. (2004). Briefly, HEK293T cells were transfected with pRK5 constructs using Lipofectamin2000 (Invitrogen). Twenty-two hours post-transfection, cells were harvested and lysed in TNE₁₅₀ buffer (20 mM Tris-HCl at pH 8.0, 150 mM NaCl, 1 mM EDTA, 1 mM PMSF, protease inhibitor cocktail) containing 1% Triton X-100 for 40 min on ice. The lysate was cleared by centrifugation at 14,000g for 10 min at 4°C, and the resulting supernatant was mixed with rabbit anti-HA (Abcam), followed by addition of Protein A-agarose beads (Amersham). The immunoprecipitates were analyzed by SDS-PAGE followed by immunoblot using anti-myc (9E10; 1:250).

GST pull-down assay

GST fusion constructs (GST-UNC-76 [full-length] or GST-KHC [amino acids 675–975]) (Gindhart et al. 2003) were introduced into *E. coli* strain BL21 (Stratagene) and protein expression was induced by 3% The Inducer (Molecular, Inc.), an analog of isopropyl- β -D-thiogalactopyranoside. The expressed protein was purified on Glutathione-Sepharose 4B beads. C'-terminal UNC-51 (amino acids 557–855) was produced by in vitro transcription/translation (Promega) and applied to the GST column. UNC-76 and Syt-1 were expressed in HEK293T cells and applied to the column. The bound protein was analyzed by SDS-PAGE, followed by immunoblot.

Mass spectrometry

HA-UNC-76 and myc-UNC-51 were cotransfected into HEK293T cells. Expressed UNC-76 was purified with anti-HA, resolved by SDS-PAGE and visualized by Sypro-Ruby staining (Molecular Probes). Phosphorylated (supershifted) UNC-76 was excised from the gel, reduced with dithiothreitol, alkylated with iodoacetamide, and digested with trypsin (modified sequencing grade; Promega). Extracted peptides were analyzed by LC/MS³ for phosphorylated residues following methods described in Gruhler et al. (2005). In brief, samples were HPLC separated using a NanoLC-2D HPLC system (Eksigent Technologies) with a 300- μ m ID \times 5-mm trapping column (PepMap C₁₈, Dionex) and a 75- μ m ID \times 10-cm analytical column home packed with 3- μ m C₁₈ silica (Pursuit, Varian). Eluted peptides were sprayed directly into a LTQ-FT mass spectrometer (ThermoElectron). Full mass scans were generated using the high-resolution FT-ICR section of the instrument. Up to five ions from each full scan that exceeded a preset threshold were analyzed by MS/MS in the linear ion trap section. Fragment ions corresponding to a strong loss of phosphoric acid were automatically analyzed by MS³. Tandem mass spectra were extracted from the raw data files using the manufacturer-provided program (extract_msn.exe) and searched against the SwissProt database with the UNC-76 sequence appended using Sequest (ThermoElectron), assuming trypsin specificity, complete alkylation of cysteine, possible oxidation of methionine, and possible phosphorylation of serine, threonine, and tyrosine. MS³ spectra were extracted using msxml2other.exe (<http://sashimi.sourceforge.net>) and searched using Sequest and the same parameter set as used for the MS², except that dehydration at

serine and threonine was considered instead of phosphorylation.

MT–kinesin cosedimentation assay

MT–kinesin cosedimentation assay was done essentially as described in Saxton et al. (1988). In brief, third instar larvae were homogenized in ice-cold MT assembly buffer (0.1 M Pipes at pH 6.9, 0.9 M glycerol, 5 mM EGTA, 0.5 mM EDTA, 2.5 mM MgSO₄) supplemented with one time protease inhibitor cocktail. The homogenate was centrifuged at 15,000g for 20 min, and then at 30,000g for 30 min to remove insoluble materials. MT polymerization was induced by adding 0.3 mM GTP and 20 μM Taxol to the supernatant and incubated for 20 min at room temperature. The MT suspensions were incubated an additional 10 min with 2.5 mM AMP-PNP and 2.5 mM MgSO₄. MTs were then sedimented through a sucrose cushion (20% sucrose, 10 μM Taxol, 0.3 mM GTP in assembly buffer) at 23,000g for 50 min, washed once, and subjected to immunoblot analyses using anti-KHC (1:1,000, rabbit polyclonal; Cytoskeleton, Inc.), mouse anti-β-Tubulin (E7) (1:100; DSHB) and anti-Syt-1 (1:5,000, rabbit polyclonal; gift of Noreen Reist) (Mackler et al. 2002).

In vitro kinase assay

Wild-type or kinase-deficient UNC-51/K38A was transiently transfected into HEK293T cells. The resulting cell lysates were immunopurified with anti-HA and used for in vitro kinase assays in the presence of Mg²⁺, [γ-³²P]-ATP and His-UNC-76 as described previously (Tomoda et al. 1999). Samples were separated on 10% SDS-PAGE and autoradiographed. Immunoprecipitated samples were probed with anti-HA as a loading control. His-tagged UNC-76 was stained with Coomassie Brilliant Blue staining to confirm equal loading.

EM

Larvae were dissected in PBS and fixed in PLP fixative for 1.5 h, followed by successive incubations in 5% and 10% sucrose for 30 min at room temperature, 20% sucrose for 1 h at room temperature, and 30% sucrose overnight at 4°C. All sucrose solutions were in 0.1 M phosphate buffer (pH 7.4). The fixed larvae were washed several times with PBS, treated with 150 mM glycine in PBS for 5 min, blocked in 5% normal goat serum in PBSS (PBS + 0.1% saponin), and incubated overnight at 4°C with antibodies in the blocking buffer. After four washes of 5 min each in PBS, the larvae were incubated with secondary antibody (biotin-conjugated anti-rabbit or anti-guinea pig IgG antibody, 1:1000; Vector Laboratories) for 2 h. After five washes in PBS, they were incubated in avidin–biotin complex solution (ABC Elite; Vector Laboratories) for 1 h. They were then fixed in 0.5% glutaraldehyde in PBS for 5 min, washed five times, and incubated in the reaction solution (0.05% diaminobenzidine, 0.01% H₂O₂ in Tris-HCl buffer at pH 7.6). The specimens were processed for EM using standard techniques as described in Suzuki and Hirose (1994).

FRET

Expression constructs were made in the pRK5 vector by fusing UNC-76 in-frame with Venus (YFP) and fusing Syt-1 in frame with Cerulean (CFP). COS7 cells were transfected with expression constructs and FRET was measured 12–16 h after transfection. We used the acceptor photobleaching method to determine efficiency of FRET (Van Munster et al. 2005; Dinant et al.

2008). In our study, two-photon excited fluorescence spectra were taken before and after photobleaching of acceptor molecules (Venus) of the FRET pair. In case of efficient FRET, photobleaching of the acceptor (Venus) will lead to an increase of donor (Cerulean) fluorescence, as it is no longer quenched by the acceptor. The in situ spectroscopy was performed with a Zeiss LSM 510 NLO Meta microscope (Carl Zeiss, Inc.) equipped with Ti-Sapphire Chameleon Ultra femtosecond pulsed laser (Coherent, Inc.) as the excitation source. Excitation wavelength used was 810 nm (LaMorte et al. 2002). Average peak values for 476 nm (Cerulean) were used in calculating the FRET efficiency (KaleidaGraph, version 4.0, Synergy Software). Acceptor photobleaching was performed by scanning the field with CW 488 nm laser for 1 min. The increase in the 476-nm peak intensities after acceptor bleaching above the level of initial value for an individual cell is indicative of FRET and a protein–protein interaction. The amount of FRET was calculated as percentage of change of donor's fluorescence, compared with initial value as

$$F(\%) = (D_{ab} - D_{init}) / D_{init} * 100,$$

where D_{init} and D_{ab} are peak fluorescence intensities at 476 nm before and after acceptor photobleaching.

Acknowledgments

We thank Troy Littleton, Hugo Bellen, Bill Saxton, Christoph Schuster, Larry Goldstein, Helmut Krämer, Noreen Reist, Bloomington Stock Center, and Hybridoma Bank for reagents; Mary Young and Roger Moore for mass spectrometric analysis; Akinao Nose for advice; Ryan Lim, Satoki Umezawa, and Yasushi Maruyama for technical assistance, and Angus Nairn, Bill Saxton, Gian Garriga, Ken-ichi Ogura, Mike Barish, Paul Salvaterra, Tom Schwarz, Tom Südhof, Yasushi Ishihama, and Keely Walker for comments or reading the manuscript. T.T. is indebted to Mary Beth Hatten for her continuous support. This work was supported by Beckman start-up funds to T.T.; Grants-in-Aid for Scientific Research from MEXT, JSPS, and the Tsukuba Advanced Research Alliance (TARA) to K.F.T.; NSF award #0342761 to J.G.G.; Grant-in-Aid for Scientific Research (C) from JSPS to E.S.; NIH P41-RR01192 to T.B.K. and V.J.L.; HHMI Undergraduate Research Fellowship to R.J.; and Atsushi Kitaueda Memorial Foundation to H.T. Fly genetics and image acquisition were done by H.M. Biochemistry and molecular biology was done by H.T. and R.F. Time-lapse imaging was done by H.T. EM was done by E.S. FRET was done by T.B.K. and V.J.L. R.J. and J.G.G. contributed important reagents and participated in discussion. T.T. and K.F.T. designed the experiments and wrote the manuscript.

References

- Ahantarg, A., Chadwell, L.V., Terrazas, I.B., Garcia, C.T., Nazarian, J.J., Lee, H.K., Lundell, M.J., and Cassill, J.A. 2008. Molecular characterization of Pegarn: A *Drosophila* homolog of UNC-51 kinase. *Mol. Biol. Rep.* doi: 10.1007/s11033-008-9314-4.
- Barkus, R.V., Klyachko, O., Horiuchi, D., Dickson, B.J., and Saxton, W.M. 2008. Identification of an axonal Kinesin-3 motor for fast anterograde vesicle transport that facilitates retrograde transport of neuropeptides. *Mol. Biol. Cell* **19**: 274–283.
- Blasius, T.L., Cai, D., Jih, G.T., Toret, C.P., and Verhey, K.J. 2007. Two binding partners cooperate to activate the molecular motor Kinesin-1. *J. Cell Biol.* **176**: 11–17.

- Bloom, L. and Horvitz, H.R. 1997. The *Caenorhabditis elegans* gene *unc-76* and its human homologs define a new gene family involved in axonal outgrowth and fasciculation. *Proc. Natl. Acad. Sci.* **94**: 3414–3419.
- Bloom, G.S., Richards, B.W., Leopold, P.L., Ritchey, D.M., and Brady, S.T. 1993. GTP γ S inhibits organelle transport along axonal microtubules. *J. Cell Biol.* **120**: 467–476.
- Bowman, A.B., Kamal, A., Ritchings, B.W., Philp, A.V., McGrail, M., Gindhart, J.G., and Goldstein, L.S. 2000. Kinesin-dependent axonal transport is mediated by the sunday driver (SYD) protein. *Cell* **103**: 583–594.
- Brady, S.T. 1991. Molecular motors in the nervous system. *Neuron* **7**: 521–533.
- Byrd, D.T., Kawasaki, M., Walcoff, M., Hisamoto, N., Matsu-moto, K., and Jin, Y. 2001. UNC-16, a JNK-signaling scaffold protein, regulates vesicle transport in *C. elegans*. *Neuron* **32**: 787–800.
- Coy, D.L., Hancock, W.O., Wagenbach, M., and Howard, J. 1999. Kinesin's tail domain is an inhibitory regulator of the motor domain. *Nat. Cell Biol.* **5**: 288–292.
- Dinant, C., van Royen, M.E., Vermeulen, W., and Houtsmuller, A.B. 2008. Fluorescence resonance energy transfer of GFP and YFP by spectral imaging and quantitative acceptor photobleaching. *J. Microsc.* **231**: 97–104.
- Friedman, D.S. and Vale, R.D. 1999. Single-molecule analysis of kinesin motility reveals regulation by the cargo-binding tail domain. *Nat. Cell Biol.* **1**: 293–297.
- Gindhart, J.G., Desai, C.J., Beushausen, S., Zinn, K., and Goldstein, L.S. 1998. Kinesin light chains are essential for axonal transport in *Drosophila*. *J. Cell Biol.* **141**: 443–454.
- Gindhart, J.G., Chen, J., Faulkner, M., Gandhi, R., Doerner, K., Wisniewski, T., and Nandelestadt, A. 2003. The kinesin-associated protein UNC-76 is required for axonal transport in the *Drosophila* nervous system. *Mol. Biol. Cell* **14**: 3356–3365.
- Gruhler, A., Olsen, J.V., Mohammed, S., Mortensen, P., Faergeman, N.J., Mann, M., and Jensen, O.N. 2005. Quantitative phosphoproteomics applied to the yeast pheromone signaling pathway. *Mol. Cell. Proteomics* **4**: 310–327.
- Guillaud, L., Wong, R., and Hirokawa, N. 2008. Disruption of KIF17-Mint1 interaction by CaMKII-dependent phosphorylation: A molecular model of kinesin-cargo release. *Nat. Cell Biol.* **10**: 19–29.
- Guzik, B.W. and Goldstein, L.S. 2004. Microtubule-dependent transport in neurons: Steps towards an understanding of regulation, function and dysfunction. *Curr. Opin. Cell Biol.* **16**: 443–450.
- Hackney, D.D. and Stock, M.F. 2000. Kinesin's IAK tail domain inhibits initial microtubule-stimulated ADP release. *Nat. Cell Biol.* **5**: 257–260.
- Hara, T., Nakamura, K., Matsui, M., Yamamoto, A., Nakahara, Y., Suzuki-Migishima, R., Yokoyama, M., Mishima, K., Saito, I., Okano, H., et al. 2006. Suppression of basal autophagy in neural cells causes neurodegenerative disease in mice. *Nature* **441**: 885–889.
- Hauptmann, G. and Gerster, T. 2000. Multicolor whole-mount in situ hybridization. *Methods Mol. Biol.* **137**: 139–148.
- Hedgecock, E.M., Culotti, J.G., Thomson, J.N., and Perkins, L.A. 1985. Axonal guidance mutants of *Caenorhabditis elegans* identified by filling sensory neurons with fluorescein dyes. *Dev. Biol.* **111**: 158–170.
- Hirokawa, N. 1998. Kinesin and dynein superfamily proteins and the mechanism of organelle transport. *Science* **279**: 519–526.
- Hirokawa, N. and Takemura, R. 2005. Molecular motors and mechanisms of directional transport in neurons. *Nat. Rev. Neurosci.* **6**: 201–214.
- Hollenbeck, P.J. 1993. Phosphorylation of neuronal kinesin heavy and light chains in vivo. *J. Neurochem.* **60**: 2265–2275.
- Horiuchi, D., Barkus, R.V., Pilling, A.D., Gassman, A., and Saxton, W.M. 2005. APLIP1, a kinesin binding JIP-1/JNK scaffold protein, influences the axonal transport of both vesicles and mitochondria in *Drosophila*. *Curr. Biol.* **15**: 2137–2141.
- Horiuchi, D., Collins, C.A., Bhat, P., Barkus, R.V., Diantonio, A., and Saxton, W.M. 2007. Control of a kinesin-cargo linkage mechanism by JNK pathway kinases. *Curr. Biol.* **17**: 1313–1317.
- Hurd, D.D. and Saxton, W.M. 1996. Kinesin mutations cause motor neuron disease phenotypes by disrupting fast axonal transport in *Drosophila*. *Genetics* **144**: 1075–1085.
- Kamal, A., Almenar-Queralt, A., LeBlanc, J.F., Roberts, E.A., and Goldstein, L.S. 2001. Kinesin-mediated axonal transport of a membrane compartment containing β -secretase and presenilin-1 requires APP. *Nature* **414**: 643–648.
- Klionsky, D.J. and Ohsumi, Y. 1999. Vacuolar import of proteins and organelles from the cytoplasm. *Annu. Rev. Cell Dev. Biol.* **15**: 1–32.
- Komatsu, M., Waguri, S., Chiba, T., Murata, S., Iwata, J., Tanida, I., Ueno, T., Koike, M., Uchiyama, Y., Kominami, E., et al. 2006. Loss of autophagy in the central nervous system causes neurodegeneration in mice. *Nature* **441**: 880–884.
- Kuroda, S., Nakagawa, N., Tokunaga, C., Tatematsu, K., and Tanizawa, K. 1999. Mammalian homologue of the *Caenorhabditis elegans* UNC-76 protein involved in axonal outgrowth is a protein kinase C zeta-interacting protein. *J. Cell Biol.* **144**: 403–411.
- Kurusu, M., Awasaki, T., Masuda-Nakagawa, L.M., Kawauchi, H., Ito, K., and Furukubo-Tokunaga, K. 2002. Embryonic and larval development of the *Drosophila* mushroom bodies: Concentric layer subdivisions and the role of fasciclin II. *Development* **129**: 409–419.
- Lai, T. and Garriga, G. 2004. The conserved kinase UNC-51 acts with VAB-8 and UNC-14 to regulate axon outgrowth in *C. elegans*. *Development* **131**: 5991–6000.
- LaMorte, V.J., Krasieva, T.B., and Zoumi, A. 2002. One-photon versus two-photon excited FRET of GFP fusion protein. In *Multiphoton microscopy in the biomedical sciences II*, Proc. SPIE 4620 (eds. A. Periasamy and P.T. So), pp. 73–78. The International Society for Optical Engineering, San Jose, CA.
- Lazarov, O., Morfini, G.A., Lee, E.B., Farah, M.H., Szodorai, A., DeBoer, S.R., Koliatsos, V.E., Kins, S., Lee, V.M., Wong, P.C., et al. 2005. Axonal transport, amyloid precursor protein, kinesin-1, and the processing apparatus: Revisited. *J. Neurosci.* **25**: 2386–2395.
- Liu, Z., Steward, R., and Luo, L. 2000. *Drosophila* Lis1 is required for neuroblast proliferation, dendritic elaboration and axonal transport. *Nat. Cell Biol.* **2**: 776–783.
- Mackler, J.M., Drummond, J.A., Loewen, C.A., Robinson, I.M., and Reist, N.E. 2002. The C(2)B Ca(2+)-binding motif of synaptotagmin is required for synaptic transmission in vivo. *Nature* **418**: 340–344.
- Martin, M., Iyadurai, S.J., Gassman, A., Gindhart, J.G., Hays, T.S., and Saxton, W.M. 1999. Cytoplasmic dynein, the dynactin complex, and kinesin are interdependent and essential for fast axonal transport. *Mol. Biol. Cell* **10**: 3717–3728.
- Miki, H., Okada, Y., and Hirokawa, N. 2005. Analysis of the kinesin superfamily: Insights into structure and function. *Trends Cell Biol.* **15**: 467–476.
- Morfini, G., Szebenyi, G., Elluru, R., Ratner, N., and Brady, S.T. 2002. Glycogen synthase kinase 3 phosphorylates kinesin light chains and negatively regulates kinesin-based motility. *EMBO J.* **21**: 281–293.

- Ogura, K. and Goshima, Y. 2006. The autophagy-related kinase UNC-51 and its binding partner UNC-14 regulate the subcellular localization of the Netrin receptor UNC-5 in *Caenorhabditis elegans*. *Development* **133**: 3441–3450.
- Ogura, K., Wicky, C., Magnenat, L., Tobler, H., Mori, I., Muller, F., and Ohshima, Y. 1994. *Caenorhabditis elegans* unc-51 gene required for axonal elongation encodes a novel serine/threonine kinase. *Genes & Dev.* **8**: 2389–2400.
- Ogura, K., Shirakawa, M., Barnes, T.M., Hekimi, S., and Ohshima, Y. 1997. The UNC-14 protein required for axonal elongation and guidance in *Caenorhabditis elegans* interacts with the serine/threonine kinase UNC-51. *Genes & Dev.* **11**: 1801–1811.
- Okada, Y., Yamazaki, H., Sekine-Aizawa, Y., and Hirokawa, N. 1995. The neuron-specific kinesin superfamily protein KIF1A is a unique monomeric motor for anterograde axonal transport of synaptic vesicle precursors. *Cell* **81**: 769–780.
- Pack-Chung, E., Kurshan, P.T., Dickman, D.K., and Schwarz, T.L. 2007. A *Drosophila* kinesin required for synaptic bouton formation and synaptic vesicle transport. *Nat. Neurosci.* **10**: 980–989.
- Pulipparacharuvil, S., Akbar, M.A., Ray, S., Sevrioukov, E.A., Haberman, A.S., Rohrer, J., and Krämer, H. 2005. *Drosophila* Vps16A is required for trafficking to lysosomes and biogenesis of pigment granules. *J. Cell Sci.* **118**: 3663–3673.
- Sakamoto, R., Byrd, D.T., Brown, H.M., Hisamoto, N., Matsumoto, K., and Jin, Y. 2005. The *Caenorhabditis elegans* UNC-14 RUN domain protein binds to the kinesin-1 and UNC-16 complex and regulates synaptic vesicle localization. *Mol. Biol. Cell* **16**: 483–496.
- Sato-Yoshitake, R., Yorifuji, H., Inagaki, M., and Hirokawa, N. 1992. The phosphorylation of kinesin regulates its binding to synaptic vesicles. *J. Biol. Chem.* **267**: 23930–23936.
- Saxton, W.M., Porter, M.E., Cohn, S.A., Scholey, J.M., Raff, E.C., and McIntosh, J.R. 1988. *Drosophila* kinesin: Characterization of microtubule motility and ATPase. *Proc. Natl. Acad. Sci.* **85**: 1109–1113.
- Scheinfeld, M.H., Roncarati, R., Vito, P., Lopez, P.A., Abdallah, M., and D'Adamio, L. 2002. Jun NH₂-terminal kinase (JNK) interacting protein 1 (JIP1) binds the cytoplasmic domain of the Alzheimer's β -amyloid precursor protein (APP). *J. Biol. Chem.* **277**: 3767–3775.
- Scott, R.C., Schuldiner, O., and Neufeld, T.P. 2004. Role and regulation of starvation-induced autophagy in the *Drosophila* fat body. *Dev. Cell* **7**: 167–178.
- Scott, R.C., Juhasz, G., and Neufeld, T.P. 2007. Direct induction of autophagy by atg1 inhibits cell growth and induces apoptotic cell death. *Curr. Biol.* **17**: 1–11.
- Stowers, R.S., Megeath, L.J., Gorska-Andrzejak, J., Meinertzhagen, I.A., and Schwarz, T.L. 2002. Axonal transport of mitochondria to synapses depends on milton, a novel *Drosophila* protein. *Neuron* **36**: 1063–1077.
- Südhof, T.C. 2004. The synaptic vesicle cycle. *Annu. Rev. Neurosci.* **27**: 509–547.
- Suzuki, E. and Hirosawa, K. 1994. Immunolocalization of a *Drosophila* phosphatidylinositol transfer protein (rdgB) in normal and *rdgA* mutant photoreceptor cells with special reference to the subrhabdomeric cisternae. *J. Electron Microsc. (Tokyo)* **43**: 183–189.
- Tomoda, T., Bhatt, R.S., Kuroyanagi, H., Shirasawa, T., and Hatten, M.E. 1999. A mouse serine/threonine kinase homologous to *C. elegans* UNC51 functions in parallel fiber formation of cerebellar granule neurons. *Neuron* **24**: 833–846.
- Tomoda, T., Kim, J.-H., Zhan, C., and Hatten, M.E. 2004. Role of Unc51.1 and its binding partners in CNS axon outgrowth. *Genes & Dev.* **18**: 541–558.
- Torroja, L., Chu, H., Kotovsky, I., and White, K. 1999. Neuronal overexpression of APPL, the *Drosophila* homologue of the amyloid precursor protein (APP), disrupts axonal transport. *Curr. Biol.* **9**: 489–492.
- Vale, R.D. 2003. The molecular motor toolbox for intracellular transport. *Cell* **112**: 467–480.
- Vallee, R.B. and Sheetz, M.P. 1996. Targeting of motor proteins. *Science* **271**: 1539–1544.
- Van Munster, E.B., Kremers, G.J., Adjobo-Hermans, M.J., and Gadella Jr., T.W. 2005. Fluorescence resonance energy transfer (FRET) measurement by gradual acceptor photobleaching. *J. Microsc.* **218**: 253–262.
- Verhey, K.J., Meyer, D., Deehan, R., Blenis, J., Schnapp, B.J., Rapoport, T.A., and Margolis, B. 2001. Cargo of kinesin identified as JIP scaffolding proteins and associated signaling molecules. *J. Cell Biol.* **152**: 959–970.
- Zhang, J., Schulze, K.L., Hiesinger, P.R., Suyama, K., Wang, S., Fish, M., Acar, M., Hoskins, R.A., Bellen, H.J., and Scott, M.P. 2007. Thirty-one flavors of *Drosophila* rab proteins. *Genetics* **176**: 1307–1322.
- Zhou, X., Babu, J.R., da Silva, S., Shu, Q., Graef, I.A., Oliver, T., Tomoda, T., Tani, T., Wooten, M.W., and Wang, F. 2007. Unc-51-like kinase 1/2-mediated endocytic processes regulate filopodia extension and branching of sensory axons. *Proc. Natl. Acad. Sci.* **104**: 5842–5847.
- Zinsmaier, K.E., Eberle, K.K., Buchner, E., Walter, N., and Benzer, S. 1994. Paralysis and early death in cysteine string protein mutants of *Drosophila*. *Science* **263**: 977–980.